

Multiferroic properties of composites of PLZT and substituted CoFe_2O_4

Dipti^{a,d}, Parveen Kumar^{b,*}, J. K. Juneja^c, Sangeeta Singh^d, K. K. Raina^e and Chandra Prakash^f

^aElectro ceramic Research Lab, GVM Girls College, Sonapat-131001, India

^bDepartment of Physics, DIT University, Dehradun-248009, India

^cDepartment of Physics, PG Hindu College, Sonapat-131001, India

^dDepartment of Physics, GVM Girls College, Sonapat-131001, India

^eSchool of Physics & Materials Science, Thapar University, Patiala-147004, India

^fSolid State Physics Laboratory, Lucknow Road, Delhi-110054, India

The magnetolectric composite with composition $x\text{Co}_{0.8}\text{Ni}_{0.2}\text{Fe}_2\text{O}_4 + (1-x)\text{Pb}_{0.9925}\text{La}_{0.005}\text{Zr}_{0.55}\text{Ti}_{0.45}\text{O}_3$, $x = 0.00, 0.05, 0.10, 0.15$ and 1.00 were prepared by solid state reaction method. The structural, microstructural, dielectric, ferroelectric and magnetic properties were studied. The X-ray diffraction and Reitveld refinement of samples confirm the formation of mixed phases of tetragonal and cubic spinel structure in composite. The microstructure of composites shows the coexistence both types of grains corresponding to their phases. Frequency dependent dielectric studies at room temperature depict the decrease in dielectric constant (ϵ) and increase in tangent loss ($\tan\delta$) in composites with increase in ferrite content. P-E Hysteresis loop and M-H hysteresis loop confirms the ferroelectric and ferromagnetic nature of composites. Existence of P-E (ferroelectric) and M-H (magnetic) at room temperature confirms the multiferroicity in the composites.

Key words: Magneto electric, PLZT, Ferrite

Introduction

The magnetolectric composites of ferrite and ferroelectric phases are of great interest for studies due to existence of strain mediated magnetolectric coupling that are suitable for magnetolectric sensors, transducers, filters, memory devices and electromechanical devices [1-4]. The magnetolectric coupling is also known as ME Effect, i.e., when a magnetic field is applied to the composite, the strain induced in the magnetostrictive magnetic phase is passed to the piezoelectric phase, which in turn induces an electric polarization [5]. Many composite systems of ferroelectrics (PZT, BaTiO_3 and BiFeO_3) with ferrites (CoFe_2O_4 , NiFe_2O_4 , $\text{NiZnFe}_2\text{O}_4$, MnFe_2O_4 and ZnFe_2O_4) have also been synthesized using different methods [6-9]. Mo *et al.* [10] reported the magnetic, dielectric and magnetolectric composites of La substituted BiFe_2O_3 - CoFe_2O_4 . Magnetolectric effect in $\text{Ni}_{0.8}\text{Zn}_{0.2}\text{Fe}_2\text{O}_4$ and La substituted Pb ($\text{Zr}_{0.65}\text{Ti}_{0.35}$) O_3 composites was reported by R. Rani *et al.* [11]. Fawzi *et al.* [12] have reported the magnetolectric effect in $(x)\text{Ni}_{0.8}\text{Zn}_{0.2}\text{Fe}_2\text{O}_4 + (1-x)\text{Pb}_{0.93}\text{La}_{0.07}(\text{Zr}_{0.60}\text{Ti}_{0.40})\text{O}_3$ composites. Same research group have also reported magnetolectric effect on $(x)\text{CoZnFe}_2\text{O}_4 + (1-x)\text{Pb}_{0.93}\text{La}_{0.07}(\text{Zr}_{0.60}\text{Ti}_{0.40})\text{O}_3$ [13]. Roy *et al.* [14] prepared $\text{Pb}_{0.85}\text{La}_{0.15}\text{TiO}_3$ - CoFe_2O_4 composite thin films prepared by wet chemical method and

studied the effect of on dielectric properties of the composites. There are no reports on magnetolectric effect on PLZT - CNFO composite ceramics. In this context, we are reporting the magneto electric effect in $x\text{CNFO} + (1-x)\text{PLZT}$ composites. Thus for selection of ferroelectric and ferrimagnetic materials for composites, one should choose the ferroelectric and ferrimagnetic material of higher resistivity, proper mole ratio of both the phases and high magnetostriction & piezoelectric coefficient. For this, PLZT has been chosen as ferroelectric phase as La substituted PZT not only increase the resistivity but also improves the dielectric constant, ferroelectric properties and piezoelectric coefficient. $\text{Co}_{0.8}\text{Ni}_{0.2}\text{Fe}_2\text{O}_4$ has been selected as ferrimagnetic phase as it has higher resistivity high magnetostriction coefficient and low eddy current losses.

In the present paper, polycrystalline composites samples of $x\text{CNFO} + (1-x)\text{PLZT}$ were prepared using solid state reaction method. The structural, dielectric, ferroelectric and magnetic properties are studied with effect of CNFO (x) in detail.

Experimental

The raw materials CoCO_3 , NiO and Fe_2O_3 for CNFO phase and PbO , La_2O_3 , ZrO_2 and TiO_2 for PLZT phase are taken to prepare the composite. Appropriate amount of raw materials of corresponding phase were ball milled for 4 hrs and calcined at 900 °C and 800 °C for 4 hrs respectively. The calcined powders were again

*Corresponding author:
Tel : +91-9996660707
E-mail: parveenpaliwal@gmail.com

ball milled and recalcined at 950 °C and 800 °C for 4 hrs respectively. The mixing powers were ball milled and mixed with 3% (by weight) PVA and pressed in to pallets using uniaxial hydraulic press with 1-2 mm thickness and 15 mm diameter. Pure PLZT and CNFO were sintered at 1250 °C and 1000 °C for 4 hrs respectively, while composites were sintered at 1150 °C for 4 hrs in lead rich environment.

The phase structure of the sintered samples were determined by X-ray Diffractometer (XRD) with $\text{CuK}\alpha$ ($\lambda = 1.541 \text{ \AA}$) radiation. The dielectric properties of the samples were measured using Hioki 3532-50 LCR meter. The ferroelectric hysteresis loops of all samples except CNFO were measured by P-E loop Tracer at room temperature. The ferromagnetic hysteresis loops of composite samples were measured by vibrating sample magnetometer (Lakeshore 735 VSM, 662). The piezoelectric coefficients were determined for all samples after poling.

Result and Discussion

The X-ray Diffraction pattern of x CNFO + (1- x) PLZT, $x = 0.00, 0.05, 0.10, 0.15$ and 1.00 are shown in Figure 1. Pure PLZT sample have tetragonal structure and CNFO have spinel cubic structure and both phases are present in composites. Samples were indexed with specific indices as confirmed by JCPDS card. Absence of product phases confirmed that there is no interdiffusion between the constituent phases. With increases in ferrite content, intensity of ferrite peak at 35 ° increases as it is observed in XRD pattern.

FULLPROF software was used to study the Reitveld analysis of all samples. Single phase model corresponding to ferroelectric phase with space group $P4mm$ was carried out in Reitveld refinement analysis with the presence of weak peaks, corresponding to ferrite phase in the composites. Ferrite peaks were distinguished in refined pattern and shown by symbol '#'. Experimental data (observed) are shown by circle while calculated are shown by solid lines. From XRD pattern, it is observed that experimental and calculated pattern are approximately fitted with small values of goodness of fit (χ^2). Lattice parameters of ferroelectric phase, were calculated from refined XRD pattern. Lattice parameters corresponding to ferrite phase increases, with increase in ferrite content in the composite.

The effect by La substitution in ferroelectric phase and by variation of ferrite content (CNFO) on the morphology and shapes of the composites grain were studied by SEM analysis. The SEM images of x CNFO + (1- x) PLZT, $x = 0.00, 0.05, 0.10, 0.15$ and 1.00 are shown in Figure 2. Average grain size of the composites was determined from linear intercept method. With increase the ferrite content in the composites, average grain size of the composites increases with increase in ferrite content. The values of average grain size with x

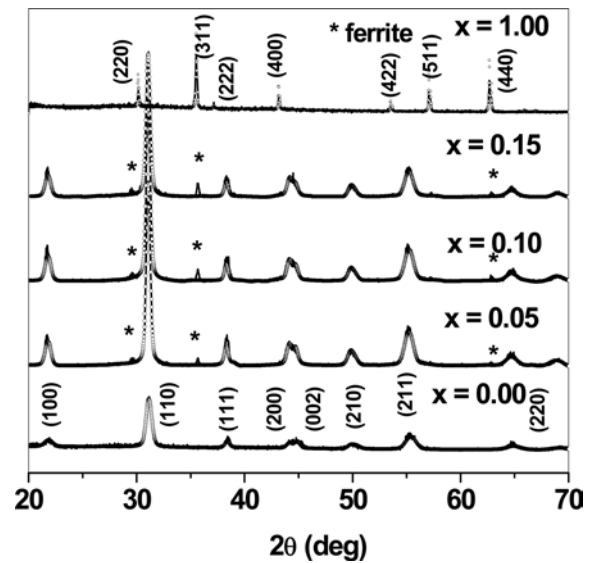


Fig. 1. XRD diffraction pattern of all samples.

Table 1. Lattice Constants, Exp. Density, X -Ray and Relative density for all values of x .

Parameters/ x	0.00	0.05	0.10	0.15
(CNFO phase) a (Å)	–	8.35929	8.3687	8.3894
(PLZT phase) a (Å)	4.05613	4.05276	4.05213	4.05375
c (Å)	4.10786	4.10369	4.10236	4.10025
c/a	1.01275	1.01256	1.01239	1.01147
Exp. Density (g/cc)	6.9357	6.9689	6.4324	6.8050
X-Ray density (g/cc)	7.5134	7.9461	7.81077	7.66535
Relative density (%)	89.563	87.802	82.3526	88.7768

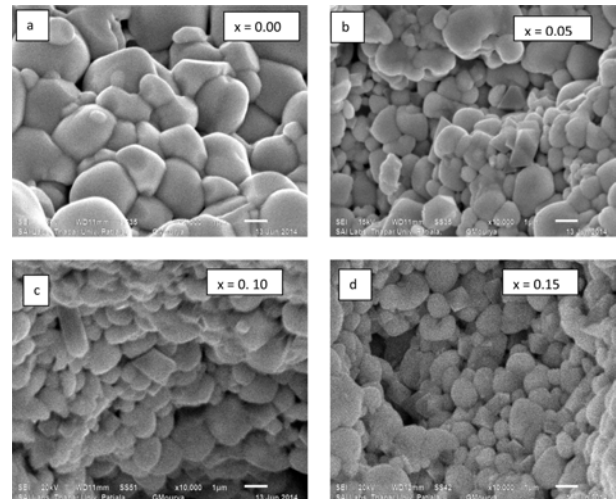


Fig. 2. SEM micrograph for all samples.

$= 0.00, 0.05, 0.10$ and 0.15 are 1.66, 0.935, 0.967 and 1.014 μm respectively. Theoretical density was measured from X-Ray Diffraction pattern. Experimental density was measured from Archimedes principle. The values of experimental, theoretical and relative densities are given in Table1. The relative density of composite samples decreases with increase in ferrite content. This is

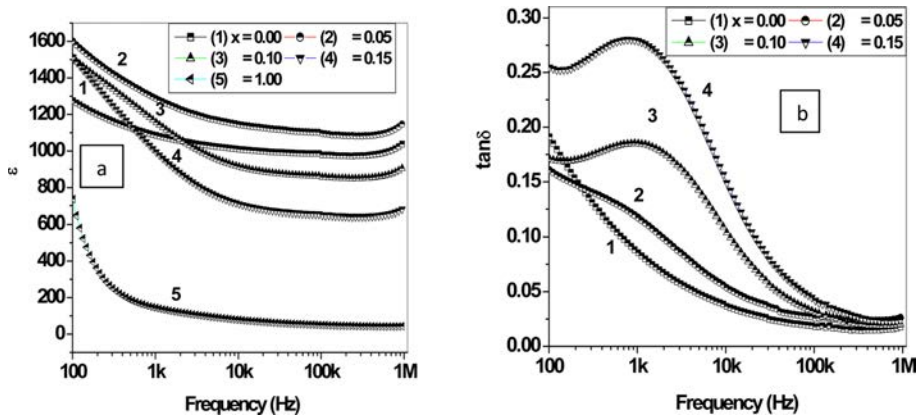


Fig. 3. Dielectric constant and tangent loss with frequency for all samples.

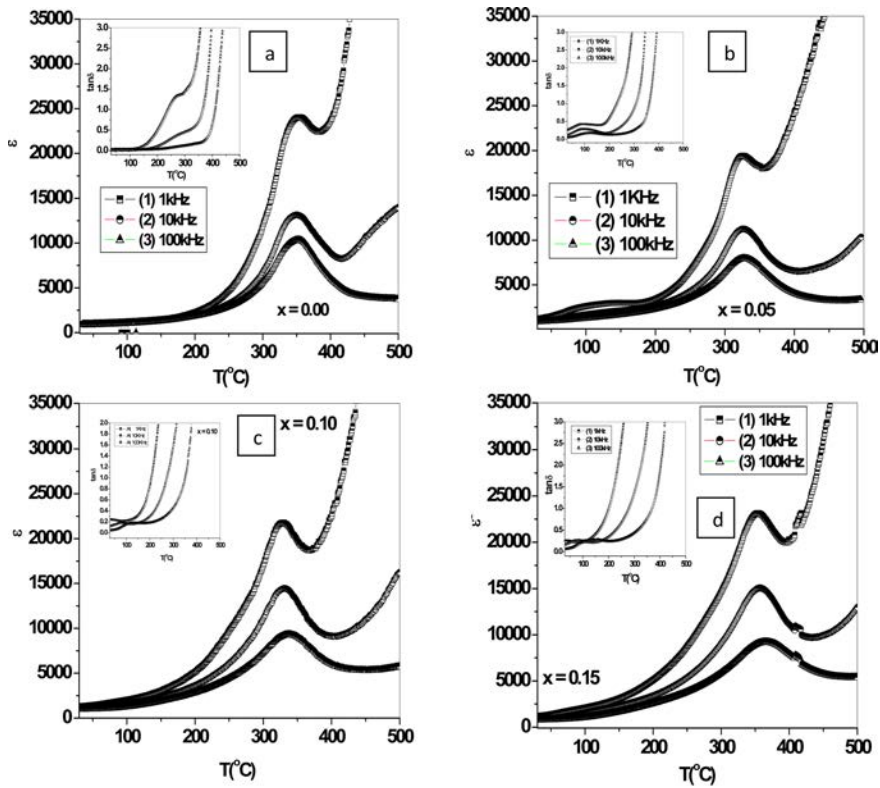


Fig. 4. (a-d) Variation of dielectric constant as function of temperature at 1 kHz, 10 kHz and 100 kHz. Inset shows the variation of loss tangent with temperature.

observed due to lower density of CNFO phase. The higher values are observed for $x = 0.15$, this may be due to better sinterability and compactness.

The variation of dielectric constant (ϵ) and tangent loss ($\tan\delta$) for all samples are shown in Figure 3. The dielectric constant is higher at lower frequency then rapidly decreasing with increasing frequencies and become constant at higher frequencies. Dielectric dispersion is also observed at lower frequencies. This can be explained Maxwell-Wagner Polarization with Koop's phenomenological theory [18-20]. Dipoles cannot follow the frequency of applied electric field at higher frequency so dielectric constant becomes constant or at higher frequencies, ionic and dipolar polarization decreases only

electronic polarization dominant. As observed in Figure 3, the dielectric constant of pure PLZT is higher and CNFO have lower dielectric constant at 100 Hz. Reversible behavior is observed in $\tan\delta$ in PLZT and CNFO sample. A relaxation peak is observed in CNFO sample. In composites of (x) CNFO + $(1-x)$ PLZT, we observed that the values of dielectric constant of composites are higher at lower frequency. This higher polarization is due to two effects: (1) space charge polarization due to inhomogeneous dielectric structure. The inhomogeneities present in the system are impurities and porosities etc [15]. (2) Ferroelectric regions are surrounded by non-ferroelectric (ferrite) which causes the accumulation of charges at their grain boundary [15-17]. With increase in ferrite content

Table 2. Dielectric properties of x CNFO-(1-x) PLZT composite samples.

x	ϵ_{RT}	$T_c(^{\circ}\text{C})$	ϵ_{Tc}	$\tan\delta_{RT}$	$\tan\delta_{Tc}$
0.00	927	352	10342	0.027	0.178
0.05	906	327	7958	0.038	0.382
0.10	976	337	9305	0.040	0.781
0.15	782	365	9199	0.060	0.948

in composites, dielectric constant decreases. This may be due to lower dielectric constant of dielectric constant of CNFO as compared to PLZT. Tangent loss of composite samples has show similar dispersion as observed in variation of dielectric constant with frequency. It is observed that with increase in ferrite content from $x = 0.05$ to 0.15 in step of 0.05, loss increases which is attributed due to high conductivity of ferrite phase. With ferrite addition, peak is also observed in all composite samples and this peak is also shifted to lower frequency side with increase in ferrite content in composites. This peak is observed when hopping frequency of ions of different valance state matches with frequency of applied electric field [21, 22].

The variations of dielectric constant (ϵ) with temperature at 1 kHz, 10 kHz and 100 kHz for all samples are shown in Figure 4 (a-d) with inset showing loss tangent ($\tan\delta$).

All samples show normal ferroelectric behavior and show the ferroelectric-paraelectric phase transition. Room temperature dielectric constant decreases with increase in ferrite content in composite. This is due to low dielectric constant of CNFO phase than that of PLZT phase. Curie temperature of composite sample is found to increase with increase the ferrite substitution in composite which can be related with c/a ratio. It has also been observed due to magnetoelectric coupling. Similar behavior has been reported in x CFO- (1-x) PCT multiferroic system and in (1-x) BST -x CFO [23, 24]. Maximum dielectric constant decreases for $x = 0.05$ and then increases with increase in ferrite content i.e. $x = 0.10$ and 0.15. This decrease in maximum dielectric constant is due to doping effect of ferrite addition in composites.

At higher temperature (in the paraelectric region), dielectric constant increases at 1 kHz and decreases at higher frequencies (10 kHz and 100 kHz). This can be related with low frequency relaxation process [25]. This increase in dielectric constant is observed due to increase in dielectric polarization which is a result of hopping of ions in ferrite phase [26]. The variation of Loss tangent with temperature at three different frequencies is shown in inset of Figure 4. Loss peaks is observed at lower temperature as observed from the Figure. These peaks shift towards higher temperature side with increase in frequency, shows thermally activated

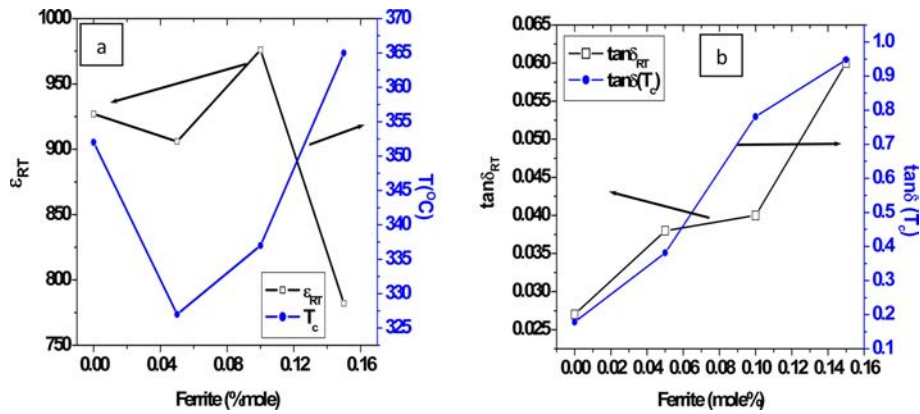


Fig. 5. Dielectric parameters of x PLZT + (1-x) CNFO composite.

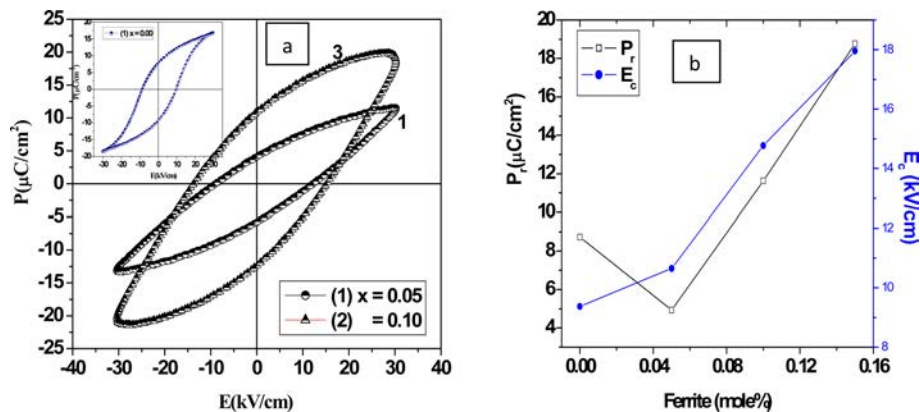


Fig. 6. (a) P-E Hysteresis loops for $x = 0.05$ and $x = 0.10$ with inset $x = 0.00$ (PLZT) (b) Dependence of ferroelectric parameters with ferrite content.

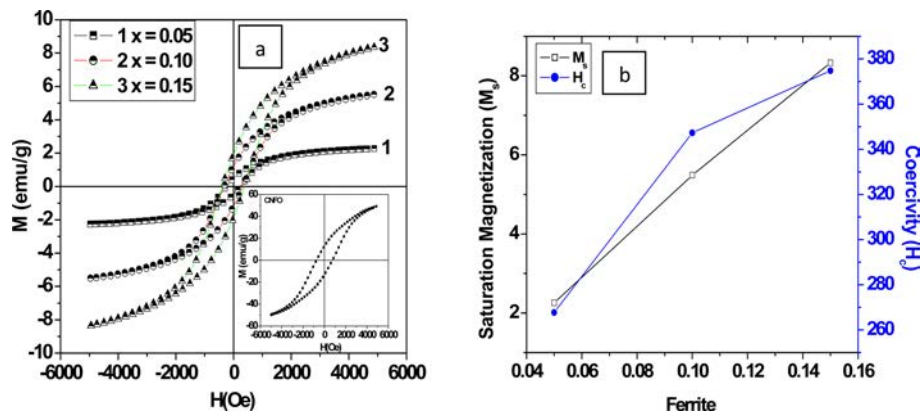


Fig. 7(a). M-H Hysteresis loops of composites sample at room temperature with inset showing CNFO. Figure 7(b) variation of saturation magnetization (M_s) and coercive field with ferrite content.

relaxation process. Loss increases at higher temperature due to space charge conduction and thermal conductivity losses. Variation of room temperature dielectric constant and Curie temperature with ferrite content is shown in Figure 5(a). The dielectric loss at room temperature and loss at Curie temperature are found to increase with increase in ferrite content as shown in Figure 5(b).

The ferroelectric nature of composites is determined by P-E hysteresis loops. Figure 6 (a) shows the ferroelectric P-E hysteresis loops for composite samples with 5% and 10% ferrite content with inset shows the P-E hysteresis loop for pure PLZT. P-E loop for PLZT is saturated while composites are not saturated. The P-E loop for $x = 0.15$ is not shown the figure because of higher value of saturation polarization (P_s -27.127 $\mu\text{C}/\text{cm}^2$). The value of remnant polarization (P_r) obtained for $x = 0.05$ is 10.65 $\mu\text{C}/\text{cm}^2$ and increased up to 18.77 $\mu\text{C}/\text{cm}^2$ for $x = 0.15$. This is due to higher value of $\tan\delta$ which dilutes the ferroelectric properties and creates the space charge across the ferroelectric phase [27]. P-E loop area of composites increases with increase in ferrite content which is due to decreasing the resistivity of composites. Similar behavior has also been reported in literature [23, 24]. The dependence of ferroelectric parameters, i.e., the remnant polarization (P_r) and coercive field (E_c) with varying ferrite content is shown in Figure 6(b). It is observed that coercive field is found to increase with increase in ferrite content. This is observed due to hindered and pinned domain wall motion of ferroelectric regions in existence of ferrite phase [28].

The M-H Hysteresis loops for composite samples with varying ferrite content are shown by Figure 7(a) with inset showing M-H loop for pure CNFO. Existence of M-H loops in composites confirms the magnetic nature of composite. All M-H loops are well saturated. With increase in ferrite content, the magnetic field at which saturation is obtained, increases. Magnetic parameters such as remnant magnetization (M_r), coercive field (H_c) and saturation magnetization (M_s) are determined from M-H hysteresis loops. The observed values for

Table 3. Ferroelectric and magnetic properties of all samples.

Parameters/x	0.00	0.05	0.10	0.15	1.00
P_r ($\mu\text{C}/\text{cm}^2$)	8.725	4.925	11.63	18.77	–
E_c (kV/cm)	9.37	10.65	14.77	17.96	–
P_s ($\mu\text{C}/\text{cm}^2$)	17.841	12.532	20.734	27.127	–
M_r (emu/g)	–	0.4739	1.2345	1.9842	13.08
M_s (emu/g)	–	2.2572	5.488	8.3295	49.45
H_c (Oe)	–	267.673	347.289	374.742	724
d_{33} (pC/N)	120	111	86	65	–

remnant polarization (M_r) are found to be 0.438, 1.235 and 1.984 (emu/g) for 5%, 10% and 15% ferrite content. The variation of magnetic parameters with ferrite content is shown in Figure 7(b). Saturation magnetization (M_s) and Coercive field (H_c) shows increasing trend with increase in ferrite content and lower than the pure CNFO (Saturation magnetization (M_s -49.45 emu/g) and Coercive field (H_c -724Oe)). This is observed due to presence of PLZT (ferroelectric phase) in the composite which act as non magnetic phase, resulting in reduction of magnetic component [29]. Therefore contribution of magnetization in composites is mainly due to present magnetic CNFO phase. The ferroelectric grains of PLZT separate the magnetic grains of CNFO phase resulting into weakening of the exchange coupling between them [30].

Conclusions

The magnetolectric composite with composition $x\text{Co}_{0.8}\text{Ni}_{0.2}\text{Fe}_2\text{O}_4 + (1-x)\text{Pb}_{(1.0125)}\text{La}_{0.005}\text{Zr}_{0.55}\text{Ti}_{0.45}\text{O}_3$ were prepared by solid state reaction method. The microstructure of composites shows the coexistence both types of grains corresponding to their phases. P-E Hysteresis loop and M-H hysteresis loop confirms the ferroelectric and ferromagnetic nature of composites. Existence of P-E (ferroelectric) and M-H (magnetic) at room temperature confirms the multiferroicity in the composites.

References

1. F. Scott, Data storage: Multiferroic memories, *Nat. Mater.* 6 (2007) 256.
2. M. Gajek, M. Bibes, S. Fusil, K. Bouzehiuan, J. Fontcuberta, A. Berthelemy, A. Fert, *Nat. Mater.* 6 (2007) 296.
3. M. Vopsaroiu, J. Blackburn, A. Muniz-Piniella, M.G. Cain, *J. Appl. Phys.* 103 (2008) 07F506.
4. S. Dong, J.F. Li, D. Viehland, *Appl. Phys. Lett.* 85 (2004) 2307.
5. R.C. Kambale, Y.A. park, N. Hur, *J. Koorean Physical Soc.* 59 (2011) 3385.
6. T.G. Lupeiko, I.V. Lisnevskaya, B.I. Zvyagintsev, *Inorg. Mater.* 31 (1995) 1139.
7. K. Uchino, *Ferroelectric Devices*, New York, Marcel Dekker, Inc. (2000).
8. S. Priya, D.J. Inman, *Energy Harvesting Technologies, Literary and Linguistic Computing* (2009).
9. R.F. Zhang, C.Y. Deng, L. Ren, Z. Li, J. P. Zhou, *Mater. Res. Bull.* 48 (2013) 4100.
10. H. Mo, D. Jiang, C.Wang, W. Zhang, J. Jiang, , *J. Alloys Compd.* 579 (2013) 187.
11. R. Rani, J.K. Juneja, S. Singh, K.K. Raina, C. Prakash, *J. Magn. Mag. Mater.* 325 (2013) 47
12. A.S. Fawzi, A.D. Sheikh, V.L. Mathe., *J. Alloys Compd.* 493 (2010) 601.
13. A.S. Fawzi, A.D. Sheikh, V.L. Mathe., *Mater. Res. Bull.* 45 (2010) 1000.
14. S. Roy, S.B. Majumder, *Phys. Lett. A.* 375 (2011) 1538.
15. M.A.E. Hiti, *J. Magn. Magn. Mater.* 164 (1996) 87-96.
16. K.K. Patankar, S.A. Patil, K.V. Sivakumar, R.P. Mahajan, Y.D. Kolekar, M.B. Kothale, *Mater. Chem. Phys.* 65 (2000) 97.
17. K.K. Patankar, S.S. Joshi, B.K. Chougule, *Phys. Lett. A* 346 (2005) 337.
18. C.G. Koops, *Phys. Rev. B* 83 (1951) 121.
19. J.C. Maxwell, *Electricity and Magnetism*, Oxford Univ. Press, London (1973).
20. K.W. Wagner, *Ann. Phys.* 40 (1993) 817.
21. A.M. Abdeen, O.M. Hameda, E.E. Assem, M.M. El-Sehly, *J. Magn. Magn. Mater.* 238 (2002) 75.
22. C.W. Beier, M.A. Cuevas, R.L. Brutchey, *J. Mater. Chem.* 20 (2010) 5074.
23. Y. Wang, W. Rao, M. Wang, G. Li, Y. Li, J. Gao, W. Zhou, J. Yu, *J. Mater. Sci: Mater Electron.* 23 (2012) 1064.
24. A. Sharma, R.K. Kotnala, N.S. Negi, *J. Alloys. Compd.* 582 (2013) 628.
25. A.P. Barranco, J.D.S. Guerra, R.L. Noda and E.B. Araujo, *J. Phys. D: Appl. Phys.* 41 (2008) 215503-215507.
26. R. Rani, J.K. Juneja, K.K. Raina, C. Prakash, *J. Ceram. Processing Res.* 13 (2012) 76.
27. N.S. Negi, A.C. Restogi, *Integrated Ferroelect.* 121 (2010) 36.
28. Z. Yu, C. Ang, *J. Mater. Sci.: Mater. Electron.*, 13 (2002) 193.
29. P.A. Jadhav, M.B. Shelar, B.K. Chougule, *J. Alloys. Compd.* 479 (2009) 385.
30. P. Pahuja, R. Sharma, C. Prakash, R. P. Tandon, *Ceram. Int.* 39 (2013) 9439.